

## High-frequency ambient noise tomography of southeast Australia: New constraints on Tasmania's tectonic past

M. K. Young,<sup>1</sup> N. Rawlinson,<sup>1</sup> P. Arroucau,<sup>2</sup> A. M. Reading,<sup>3</sup> and H. Tkalčić<sup>1</sup>

Received 28 April 2011; revised 29 May 2011; accepted 1 June 2011; published 13 July 2011.

[1] The island of Tasmania, at the southeast tip of Australia, is an ideal natural laboratory for ambient noise tomography, as the surrounding oceans provide an energetic and relatively even distribution of noise sources. We extract Rayleigh wave dispersion curves from the continuous records of 104 stations with ~15 km separation. Unlike most passive experiments of this type, which observe very little coherent noise below a 5 s period, we clearly detect energy at periods as short as 1 s, thanks largely to the close proximity of oceanic microseisms on all sides. The main structural elements of the eastern and northern Tasmanian crust are revealed by inverting the dispersion curves (between 1 and 12 s period) for both group and phase velocity maps. Of particular significance is a pronounced band of low velocity, observed across all periods, that underlies the Tamar River Valley and continues south until dissipating in southeast Tasmania. Together with evidence from combined active source and teleseismic tomography and heat flow data, we interpret this region as a diffuse zone of strong deformation associated with the mid-Paleozoic accretion of oceanic crust along the eastern margin of Proterozoic Tasmania, which has important implications for the evolution of the Tasman Orogen of eastern Australia. In the northwest, a narrower low-velocity anomaly is seen in the vicinity of the Arthur Lineament, which may be attributed to local sediments and strong deformation and folding associated with the final phases of the Tyennan Orogeny.

**Citation:** Young, M. K., N. Rawlinson, P. Arroucau, A. M. Reading, and H. Tkalčić (2011), High-frequency ambient noise tomography of southeast Australia: New constraints on Tasmania's tectonic past, *Geophys. Res. Lett.*, 38, L13313, doi:10.1029/2011GL047971.

### 1. Introduction

[2] The island of Tasmania comprises the southern limit of the Tasman Orogen of southeast Australia, which formed largely as a result of subduction-accretion along the proto-Pacific margin of east Gondwana throughout the Paleozoic [Glen, 2005]. Tasmania may be divided into two basement geology domains: the Western Tasmanian Terrane (WTT) and the Eastern Tasmanian Terrane (ETT) (Figure 1) [Williams, 1989]. WTT has large areas of exposed Proterozoic basement

which contrast with the Phanerozoic rocks of the adjacent mainland Lachlan Fold Belt [Reed, 2001]. ETT, however, exhibits no evidence of Proterozoic outcrop and is predominantly Paleozoic in origin [Reed, 2001].

[3] In an attempt to elucidate the lithosphere beneath southeast Australia, including Tasmania, a transportable passive seismic array experiment known as WOMBAT commenced in 1998 [Rawlinson *et al.*, 2010]. To date over 550 stations have been installed during 13 consecutive sub-array deployments. In northern Tasmania, joint inversion of teleseismic and pre-existing wide-angle (refraction and reflection) data [Rawlinson *et al.*, 2010] has revealed a pronounced low velocity anomaly in the lower crust and lithospheric mantle near the transition between ETT and WTT. Magnetotelluric and magnetovariational studies [Parkinson *et al.*, 1988] have revealed a major conductivity anomaly in northeast Tasmania, directly in line with the Tamar River. In 2007, KUTh Energy Ltd. (www.kuthenergy.com) performed an extensive heat flow survey in east Tasmania in which a significant heat flow anomaly was discovered in a ~4,000 km<sup>2</sup> region of the southern Tamar Valley.

[4] One area of particular controversy in Tasmanian tectonics is the nature of the boundary between WTT and ETT. The limited Paleozoic surface exposure indicates that there is a broad and complex area of deformation between the distinctive outcrop of WTT and ETT [Reed, 2001], but evidence of a definite boundary remains elusive. More than two decades ago it was postulated that the Tamar River marks the approximate location of a crustal-scale suture zone [Williams, 1989] - sometimes referred to as the Tamar Fracture System - between ETT and WTT. This idea has since been questioned [Leaman *et al.*, 1994; Reed, 2001; Rawlinson *et al.*, 2010], and the observed changes in stratigraphy that gave rise to the original hypothesis are now interpreted as being related to thin-skinned (near-surface) tectonic processes [Leaman *et al.*, 1994].

[5] Cayley [2011] proposes a Cambrian to Silurian tectonic scenario in which Tasmania, the Selwyn Block of central Victoria, and adjacent oceanic plateaus are jointly interpreted as an exotic Proterozoic microcontinental block that they call "VanDieland." The block is assumed to have collided with east Gondwana along the margin south of western Victoria, Australia, and north of North Victoria Land, Antarctica, along a west-dipping subduction system in the Late Cambrian. Gibson *et al.* [2011] present a variation on this tectonic scenario in which Tasmania originated south of Victoria Land, Antarctica, thus rendering unnecessary the labeling of Tasmania as an exotic terrane. In either case, VanDieland was ultimately transferred northeast to its present position, with the Selwyn Block embedded into the Lachlan Orogen. The Selwyn Block theory resolves the problem of how to reconcile the Proterozoic basement rocks of western Tasmania with

<sup>1</sup>Research School of Earth Sciences, Australian National University, Acton, ACT, Australia.

<sup>2</sup>Center of Research Excellence in Science and Technology, North Carolina Central University, Durham, North Carolina, USA.

<sup>3</sup>School of Earth Sciences, University of Tasmania, Hobart, Tasmania, Australia.

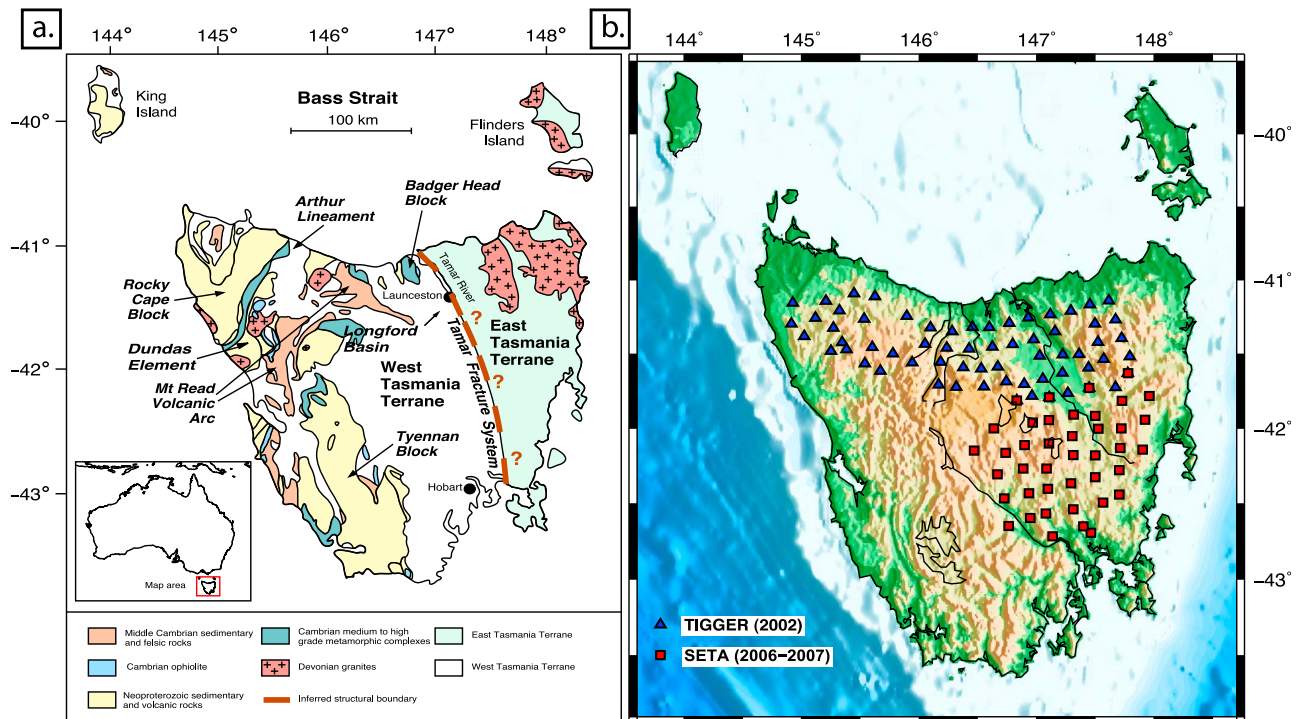


**Figure 1.** (a) Map showing the summary basement geological units of Tasmania (based on that of *Spaggiari et al.* [2003]). Only the northern portion of the boundary between WTT and ETT is exposed at the surface. The approximate location of the terrane boundary under cover is indicated by a dotted line. (b) Map of WOMBAT subarrays TIGGER and SETA used in this study.

the largely Paleozoic, oceanic crust derived Lachlan Fold Belt of Victoria.

[6] Another possibility is that WTT is one of many salients of a very irregular, rifted east Gondwana margin [*Direen and Crawford*, 2003]. Much of the Delamerian Orogen is underlain by deformed Proterozoic lithosphere, which may extend south into Tasmania, where it outcrops at the surface. In this case, the eastern edge of WTT acted as an indenter to the oceanic crust when it collided with an intraoceanic arc during the Middle Cambrian [*Direen and Crawford*, 2003]. ETT subsequently resulted from episodic accretion of oceanic crust and sediment deposition along Tasmania's eastern margin from the Silurian through Early Devonian [*Reed*, 2001].

[7] In this study, we image the crust of Tasmania using ambient seismic noise tomography applied to continuous data records extracted from the WOMBAT subarrays TIGGER and SETA. Thanks to the high station density of these arrays and prolific ocean noise from all sides [*Yang and Ritzwoller*, 2008], this is the first time that high-resolution group and phase velocity maps have been produced for Tasmania. The results from this study complement those from recent seismic and heat flow studies and lead to a substantially better understanding of the tectonic evolution of this enigmatic region of the Australian continent.

## 2. Data and Method

[8] The data for this study comes from two subarrays of the WOMBAT transportable seismic array project. The 64 short-period stations of the TIGGER array were deployed in March 2002 and span northern Tasmania, while the

40-station SETA array was installed four years later immediately south of TIGGER on the central east part of the island (Figure 1b). We use approximately seven months of data from each array to perform ambient seismic noise tomography of the region.

[9] The ambient noise cross-correlation procedure we employ is similar to that of *Bensen et al.* [2008]. To produce the highest-quality Green's functions, the noise recordings are divided up into 40 minute segments with 75% overlap. Vertical-component data is cross-correlated and stacked for all simultaneously recording station pairs, resulting in 2038 cross-correlograms for TIGGER (Figure 2a) and 779 for SETA. A phase-matched filtering process described by *Levshin and Ritzwoller* [2001] enables the utilization of cross-correlograms with a signal-to-noise ratio (SNR) as low as 3 (see *Arroucau et al.* [2010] for details), although the average SNR is 49.3 for SETA and 34.3 for TIGGER.

[10] We perform group velocity dispersion measurements using the frequency-time analysis (FTAN) method presented by *Levshin et al.* [1972] and selection criteria described by *Arroucau et al.* [2010] on the symmetric component (average of the causal and acausal signals) of the negative time derivative of the cross-correlation functions, which can be interpreted as Rayleigh wave Green's functions [*Curtis et al.*, 2006]. Phase velocities are measured using a modified version of the image transformation technique described by *Yao et al.* [2006], which invokes the far-field approximation. In order to accurately measure phase velocities up to 1 Hz, we introduce a linear-dependence of the bandpass-filter width on the central period. Both group and phase dispersion measurements are only performed when the interstation spacing is at least three wavelengths at a given period

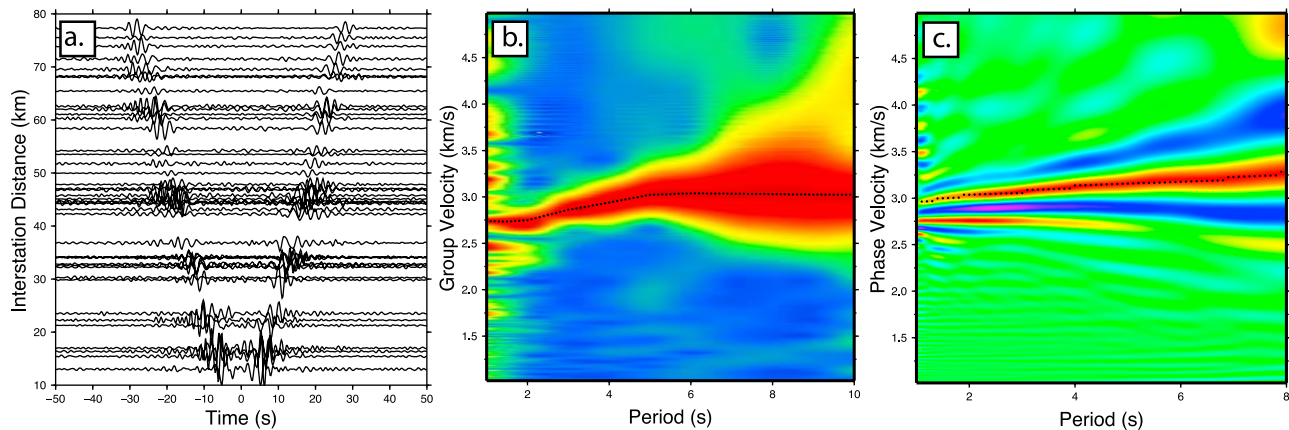


**Figure 2.** (a) Cross-correlograms calculated from the TIGGER array with respect to station TSM2. Record sections are bandpass filtered between 1 and 3 s to illustrate the clear visibility of the Rayleigh waves at high frequencies. (b) Example frequency–time diagram for the TIGGER station pair TSA4 and TSQ3 (interstation distance of 234 km). The dotted black line represents the chosen group curve for this pair. (c) Example phase velocity dispersion image for the station pair TSD2 and TSH2 (interstation distance of 63 km). The dotted black line represents the chosen phase curve for this pair.

[Bensen *et al.*, 2008]. This requirement places an upper limit on the group and phase velocity maps of about 12 s, although individual dispersion curves range up to 25 s.

[11] After making the group and phase velocity measurements (Figures 2b and 2c), a tomographic inversion is performed for periods between 1 and 12 s. Fundamental mode Rayleigh wave group and phase velocity variations are mapped on a regular grid of 3,600 nodes using an iterative, non-linear tomographic inversion scheme [Arroucau *et al.*, 2010] which uses an eikonal solver to predict traveltimes and a subspace scheme to solve the inverse problem. Both damping and smoothing regularization are applied to prevent convergence towards a solution that has unnecessarily large amplitude perturbations and model roughness. Synthetic “checkerboard” resolution tests [Rawlinson *et al.*, 2010] are performed in order to analyze the resolving power of the data. Gaussian noise with a standard deviation of 0.25 s is added to the synthetic data to simulate the noise content of the observed traveltimes.

### 3. Results

[12] Most ambient noise studies are restricted to a lower period limit of 5 to 10 s [Yao *et al.*, 2006; Bensen *et al.*, 2008; Yang *et al.*, 2007]. Moreover, studies that are able to observe coherent energy at 1 s period often lose resolution above 3 s [Huang *et al.*, 2010] due to the reduced spatial extent of their arrays. We, however, have produced group and phase velocity maps for periods between 1 and 12 s using 90% of the SETA dispersion curve measurements and 93% of those from TIGGER. Application of the tomographic inversion scheme using constant velocity starting models results in significant improvement in residual misfit for periods between 1 and 12 s, with variance reductions ranging from 24 to 88%. The lower variance reductions are associated with the longest-period (>9 s) solutions, where there is a gradual degradation of dispersion measurements as the far-field approximation becomes less accurate [Yao *et al.*, 2006].

[13] The tomography results show that there is a strong correlation between the group and phase velocity variations

across north and central east Tasmania (Figure 3). The average group and phase velocity sampling depth increases with period, with the phase velocities sampling slightly deeper than the group velocities at a given period. For typical continental crust, 1 s period surface waves are most sensitive to structure in the upper 1–2 km, whereas 12 s period surface waves are most sensitive to structure at depths between 10–15 km [Saygin and Kennett, 2010].

[14] The most obvious characteristic of the new group and phase velocity maps produced in this work, visible at all well-resolved periods, is a pronounced low-velocity zone within the neighborhood of the Tamar River Valley that continues southwards through both arrays (line A, Figure 3). This consistently broad (~50 km) feature follows a curved path that can be tracked southeast from Tasmania’s north coast before bending southward at around 42° S. Although the southern limit of the velocity images occurs at around 42.5–43° S, the low-velocity zone becomes more patchy in this area and possibly terminates near the southern border of the SETA array. We also find significantly lower velocities along the Arthur Lineament to the west (line B, Figure 3). While not as consistent as the velocity low along the Tamar River Valley, this narrower (~25 km) lineation of decreased velocities is manifest at all periods.

### 4. Discussion

[15] The pronounced low-velocity anomaly that runs approximately parallel to the Tamar River (line A, Figure 3) suggests that there is a strong change in crustal properties extending to at least 15 km depth. This low-velocity region has a width of approximately 50 km and is as much as ~0.5 km/s slower than the surrounding areas. Since the shape of this anomaly bares some similarity to the surface expression of broad-scale surface geomorphological features in northern Tasmania, we have given considerable thought to the possible influence of surface features on deeper-seated anomalies. While the low velocities at shorter periods in the northern half of the anomaly are in part due to a localised region of sedimentary rocks in the Longford Basin of north Tasmania [Direen and Leaman, 1997], the

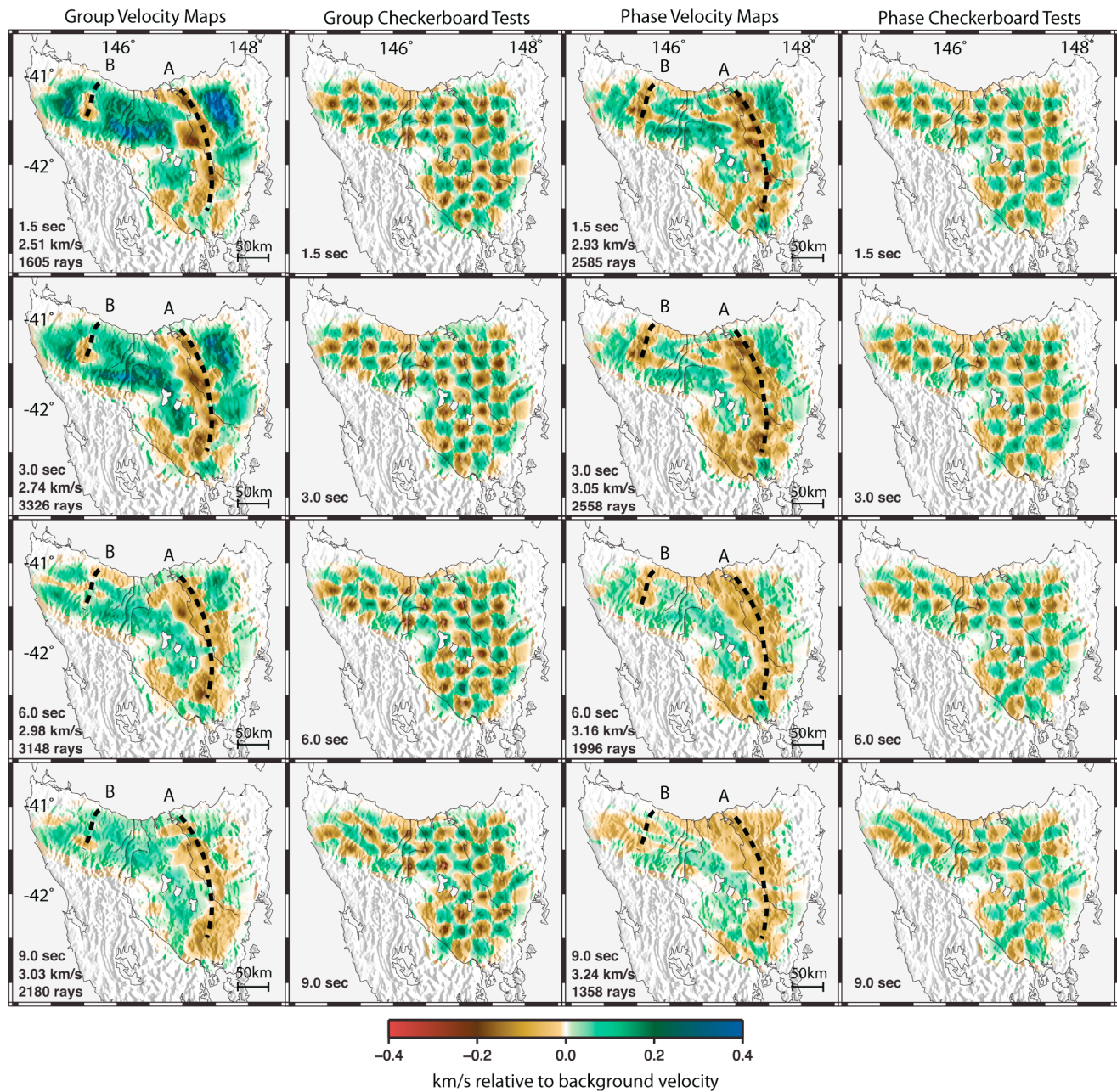


**Figure 3.** Group velocity and phase velocity maps and their corresponding checkerboard resolution tests for periods of 1.5 (top), 3.0, 6.0, and 9.0 (bottom) s. Period, background velocity, and number of ray paths are shown in the lower left corner of each panel. The input of the checkerboard tests is an alternating pattern of positive and negative velocity squares with a maximum perturbation of 0.4 km/sec. Solid black lines labeled “A” = terrane boundary zone anomaly, “B” = Arthur Lineament anomaly.

pattern observed at longer periods cannot be explained by this 800 m (maximum) surface layer of sediments. Our synthetic sensitivity kernel tests show that longer period (>4 s) velocity maps are not significantly affected by an 800 m thick low-velocity (1 km/s slower than underlying basement) sediment layer at the surface. Furthermore, the low-velocity zone extends south from the Longford Basin and is also seen down to a depth of approximately 130 km by joint wide-angle reflection, refraction, and teleseismic studies [Rawlinson *et al.*, 2010], which barely sample the upper crust in this region. The decrease in average wave-

speed that we detect is also consistent with elevated conductivity and heat flow levels that have been observed in the area [Parkinson *et al.*, 1988] ([www.kuthenergy.com](http://www.kuthenergy.com)). The new ambient seismic noise work presented here greatly improves the resolution and depth constraints of velocity variations in the Tasmanian crust.

[16] Although a definite change in crustal properties is present in the vicinity of the Tamar River, the breadth of the low-velocity anomaly precludes the presence of a lithospheric boundary resulting from the juxtaposition of two separate crustal elements. We prefer the thin-skinned scenario

as previously suggested by seismic reflection, refraction, teleseismic [Rawlinson *et al.*, 2010], and potential field data [Leaman, 1990]. A possible explanation for the unique crustal qualities of the Tamar Valley area is that the confluence of WTT and ETT once represented a passive margin between oceanic crust in the east and Proterozoic continental crust in the west [Reed, 2001].

[17] According to Reed [2001], ETT was deformed and thickened during a pre-Tabberabberan event correlating with the Benambran deformation of the Australian mainland. In this scenario, the joining of WTT and ETT corresponds to the boundary area between continental and oceanic basement, which is characterized by heavy deformation, shortening, and east-facing recumbent folds and thrusts. This explains the breadth (~50 km) of the low-velocity anomaly seen in our images (line A, Figure 3). Reed [2001] places the paleo-continent ocean boundary west of the Tamar River (corresponding to the left edge of our low-velocity zone) and assumes it continues north beneath the waters of Bass Strait and evolves into the Governor Fault in southeast Australia. Reed [2001] concludes that the boundary between ETT and WTT is equivalent to the separation of the Tabberabbera and Melbourne Zones in Victoria. This is supported by Cayley [2011] and Gibson *et al.* [2011], who argue that the rigid basement block of central Victoria (the Selwyn Block) is the northward extension of the Tasmanian Proterozoic–Early Paleozoic crust, which sits unconformably beneath sedimentary rocks of the Melbourne Zone. In this case, we would expect to see a continuation of the low-velocity anomaly through Bass Strait and into Victoria. However, to date, there have been no concurrently running arrays in Tasmania and the adjacent mainland to facilitate ambient noise imaging beneath Bass Strait. In Victoria, recent hot-spot volcanism may have influenced ambient noise group velocity maps [Arroucau *et al.*, 2010], but no analogous low-velocity zone is seen continuing through the mainland. This incongruity may suggest that some components of the Paleozoic tectonic regimes that operated in Victoria and Tasmania are not comparable.

[18] A competing hypothesis is that WTT is a salient of the eastern margin of Gondwana [Direen and Crawford, 2003]. The Proterozoic material underlying the Delamerian Orogen of Victoria is proposed to extend down through Bass Strait and into Tasmania. Western Tasmania shares many geological and petrological-geochemical similarities with western Victoria [Direen and Crawford, 2003]. Furthermore, recent teleseismic tomography of mainland southeast Australia [Rawlinson *et al.*, 2011] shows that the Delamerian Orogen extends eastward beneath the surface outcrop of the Lachlan Orogen, thereby increasing the likelihood that WTT is simply a part of Pre-Cambrian Australia. If WTT is assumed to have been a pronounced projection out from east Gondwana, then strong and concentrated deformation would be expected when the exposed margin of WTT collided with oceanic crust during the Middle Cambrian. The resulting intense deformation would be local to WTT, perhaps explaining the absence of an equivalent low-velocity zone on the mainland.

[19] Another prominent and consistent feature of the models is the low-velocity anomaly beneath the Arthur Lineament, a sheared belt of magnetic metamorphic rocks that separates the Rocky Cape Element from the Dundas Element (Figure 1a). Our maps indicate that this transition is

heavily deformed and extends at least 8 km beneath the surface. Beyond approximately 9 s period, the anomaly becomes less defined and more dispersed. The Arthur Lineament was formed during the early stages of the Tyennan Orogeny, and subsequent deformation during the Tabberabberan Orogeny resulted in further faulting, folding, and granitoid intrusion [Williams, 1989]; the lower velocities may reflect the fact that it consists mainly of metasedimentary rocks.

## 5. Conclusions

[20] In this study we obtain exceptionally high resolution Rayleigh wave fundamental mode group and phase velocity maps for periods between 1 and 12 s, thereby demonstrating that with dense seismic arrays and close proximity to oceanic microseisms, high-resolution tomography at high frequencies is possible with ambient noise methods. The resulting tomographic images of the crust across a wide range of periods reveal a ~50 km wide, southeast-trending, low-velocity lineation within the vicinity of the Tamar River. We interpret the low-velocity zone as the mid-upper crustal expression of a broad and heavily deformed transition zone, which can be attributed to the localized shortening, thickening and accretion of oceanic crust along the passive margin of WTT during the early-mid Paleozoic. The wide zone of anomalously low velocities revealed by our maps is consistent with two plate tectonic hypotheses that attempt to explain the lithospheric evolution of the region: (1) WTT can be interpreted to be part of an exotic microcontinent, inherited from the break-up of Rhodinia, that was embedded into the eastern margin of Gondwana; or (2) WTT is a salient of the eastern margin of Gondwana, and represents the southern extension of the Delamerian Orogen. In either case, it is plausible for the western margin of ETT to be represented by a broad region of strong deformation and faulting (and hence low velocity) due to the accretion of oceanic material against more rigid continental lithosphere.

[21] **Acknowledgments.** The Editor thanks Yingjie Yang and an anonymous reviewer for their assistance in evaluating this paper.

## References

- Arroucau, P., N. Rawlinson, and M. Sambridge (2010), New insight into Cainozoic sedimentary basins and Palaeozoic suture zones in southeast Australia from ambient noise surface wave tomography, *Geophys. Res. Lett.*, *37*, L07303, doi:10.1029/2009GL041974.
- Bensen, G. D., M. H. Ritzwoller, and N. M. Shapiro (2008), Broadband ambient noise surface wave tomography across the United States, *J. Geophys. Res.*, *113*, B05306, doi:10.1029/2007JB005248.
- Cayley, R. (2011), Exotic crustal block accretion to the eastern Gondwanaland margin in the Late Cambrian–Tasmania, the Selwyn Block, and implications for the Cambrian–Silurian evolution of the Ross, Delamerian, and Lachlan orogens, *Gondwana Res.*, *19*, 628–649.
- Curtis, A., P. Gerstoft, H. Sato, R. Snieder, and K. Wapenaar (2006), Seismic interferometry—Turning noise into signal, *Leading Edge*, *25*(9), 1082–1092.
- Direen, N. G., and A. J. Crawford (2003), Fossil seaward-dipping reflector sequences preserved in southeastern Australia: A 600 Ma volcanic passive margin in eastern Gondwanaland, *J. Geol. Soc.*, *160*, 985–990.
- Direen, N. G., and D. E. Leaman (1997), Geophysical modelling of structure and tectonostratigraphic history of the Longford Basin, northern Tasmania, *Explor. Geophys.*, *28*, 29–33.
- Gibson, G., M. Morse, T. Ireland, and G. Nayak (2011), Arc-continent collision and orogenesis in western Tasmanides: Insights from reactivated basement structures and formation of an ocean-continent transform boundary off western Tasmania, *Gondwana Res.*, *19*, 608–627.

- Glen, R. (2005), The Tasmanides of eastern Australia, in *Terrane Processes at the Margins of Gondwana*, edited by A. Vaughan, P. Leat, and R. Pankhurst, *Geol. Soc. Spec. Publ.*, 246, 23–96.
- Huang, Y., B. H. H. Yao, R. D. van der Hilst, W. H. K. Wen, and C. Chen (2010), Phase velocity variation at periods of 0.5–3 seconds in the Taipei Basin of Taiwan from correlation of ambient seismic noise, *Bull. Seismol. Soc. Am.*, 100, 2250–2263.
- Leaman, D. E. (1990), Inferences concerning the distribution and composition of pre-Carboniferous rocks in southeastern Tasmania, *Pap. Proc. R. Soc. Tasmania*, 124, 1–12.
- Leaman, D. E., P. W. Baillie, and C. M. Powell (1994), Precambrian Tasmania: A thin-skinned devil, *Explor. Geophys.*, 25, 19–23.
- Levshin, A. L., and M. H. Ritzwoller (2001), Automated detection, extraction, and measurement, of regional surface waves, *Pure Appl. Geophys.*, 158, 1531–1545, doi:10.1007/PL00001233.
- Levshin, A., V. F. Pisarenko, and G. A. Pogrebinsky (1972), On a frequency-time analysis of oscillations, *Ann. Geophys.*, 28, 211–218.
- Parkinson, W., R. Hermanto, J. Sayers, N. Bindoff, H. Dosso, and W. Nienaber (1988), The Tamar conductivity anomaly, *Phys. Earth Planet. Inter.*, 52, 8–22.
- Rawlinson, N., H. Tkalčić, and A. M. Reading (2010), Structure of the Tasmanian lithosphere from 3D seismic tomography, *Aust. J. Earth Sci.*, 57, 381–394.
- Rawlinson, N., B. L. N. Kennett, E. Vanacore, R. A. Glen, and S. Fishwick (2011), The structure of the upper mantle beneath the Delamerian and Lachlan orogens from simultaneous inversion of multiple teleseismic datasets, *Gondwana Res.*, 19, doi:10.1016/j.gr.2010.11.001.
- Reed, A. R. (2001), Pre-Tabberabberan deformation in eastern Tasmania: A southern extension of the Benambran Orogeny, *Aust. J. Earth Sci.*, 48, 785–7964.
- Saygin, E., and B. L. N. Kennett (2010), Ambient seismic tomography of the Australian continent, *Tectonophysics*, 481, 116–125.
- Spaggiari, C. V., D. R. Gray, D. A. Foster, and S. McKnight (2003), Evolution of the boundary between the western and central Lachlan Orogen: Implications for Tasmanide tectonics, *Aust. J. Earth Sci.*, 50, 725–749.
- Williams, E. (1989), Summary and synthesis, in *Geology and Mineral Resources of Tasmania*, edited by C. F. Burrett and E. L. Martin, *Spec. Publ. Geol. Soc. Aust.*, 15, 468–499.
- Yang, Y., and M. H. Ritzwoller (2008), Characteristics of ambient seismic noise as a source for surface wave tomography, *Geochem. Geophys. Geosyst.*, 9, Q02008, doi:10.1029/2007GC001814.
- Yang, Y., M. Ritzwoller, A. Levshin, and N. Shapiro (2007), Ambient noise Rayleigh wave tomography across Europe, *Geophys. J. Int.*, 168, 259–274.
- Yao, H., R. D. van der Hilst, and M. V. de Hoop (2006), Surface-wave array tomography in SE Tibet from ambient seismic noise and two-station analysis—I. Phase velocity maps, *Geophys. J. Int.*, 166, 732–744.

---

P. Arroucau, Center of Research Excellence in Science and Technology, North Carolina Central University, 1801 Fayetteville St., Durham, NC 27707, USA. (pierre.arroucau@anu.edu.au)

N. Rawlinson, H. Tkalčić, and M. K. Young, Research School of Earth Sciences, Australian National University, Mills Road, Bldg. 61, Acton, ACT 0200, Australia. (nicholas.rawlinson@anu.edu.au; hrvoje@rses.anu.edu.au; mallory.young@anu.edu.au)

A. Reading, School of Earth Sciences, University of Tasmania, Private Bag 79, Hobart, Tas 7001, Australia. (anya.reading@utas.edu.au)